

A Dual-Phase Coumarin Based Ratiometric Fluorescent Probe for Highly Sensitive Cyanide Sensing and Bioimaging Applications

Moumita Ghosh¹, Amitav Biswas¹, Atanu Maji¹, Subhabrata Guha², Gaurav Das², Rahul Naskar¹, Saswati Gharami^{1,*} and Tapan Kumar Mondal^{1,*}

¹Department of Chemistry, Jadavpur University, Kolkata-700 032, India.

²Department of Signal Transduction and Biogenic Amines (STBA), Chittaranjan National Cancer Institute, Kolkata- 700026, India.

E-mail: tapank.mondal@jadavpuruniversity.in

CONTENTS

Figure S1: ¹H NMR (300 MHz) spectrum of the probe (DHMH) in DMSO-d₆.

Figure S2: ¹³C NMR (101 MHz) spectrum of the probe (DHMH) in DMSO-d₆.

Figure S3: IR plot of the probe (DHMH).

Figure S4: HRMS of the probe DHMH.

Figure S5: Fluorescence emission spectra of DHMH (10 μ M) in DMSO-H₂O mixed solvents with increasing water fractions.

Figure S6: Change of emission spectra of DHMH (10 μ M) after addition of CN⁻ (20 μ M) in DMSO/H₂O (7/3, v/v) using HEPES buffered solution at pH=7.2.

Figure S7: Absorption spectra of DHMH (10 μ M) upon addition of various other anions (20 μ M) in DMSO using HEPES buffered solution at pH=7.2.

Figure S8: Change of emission spectra of DHMH (10 μ M) after addition of other anions (20 μ M) in DMSO using HEPES buffered solution at pH=7.2.

Figure S9: Mole ratio plot of DHMH.

Figure S10: The linear response curve of at emission intensity at 445 nm of DHMH depending on CN⁻ concentration.

Figure S11: Enlarged ¹H NMR spectra of the probe before and after addition of 1.0 equiv. CN⁻ in DMSO-d₆.

Figure S12: HRMS of DHMH+CN⁻.

Figure S13: pH titration plot of DHMH and DHMH+CN⁻.

Figure S14: Solid state UV spectra of DHMH and DHMH-CN⁻.

Figure S15: IR spectra of DHMH and DHMH-CN⁻.

Figure S16. Contour plots of some selected molecular orbitals of DHMH.

Figure S17. Contour plots of some selected molecular orbitals of DHMH-CN⁻.

Table S1. Vertical electronic transitions calculated by TDDFT/B3LYP/CPCM method for DHMH and DHMH-CN⁻ in DMSO.

Table S2: Lifetime decay profile of DHMH and DHMH-CN⁻.

Table S3: The comparison of the present probe (DHMH) with some previous probes for CN⁻.

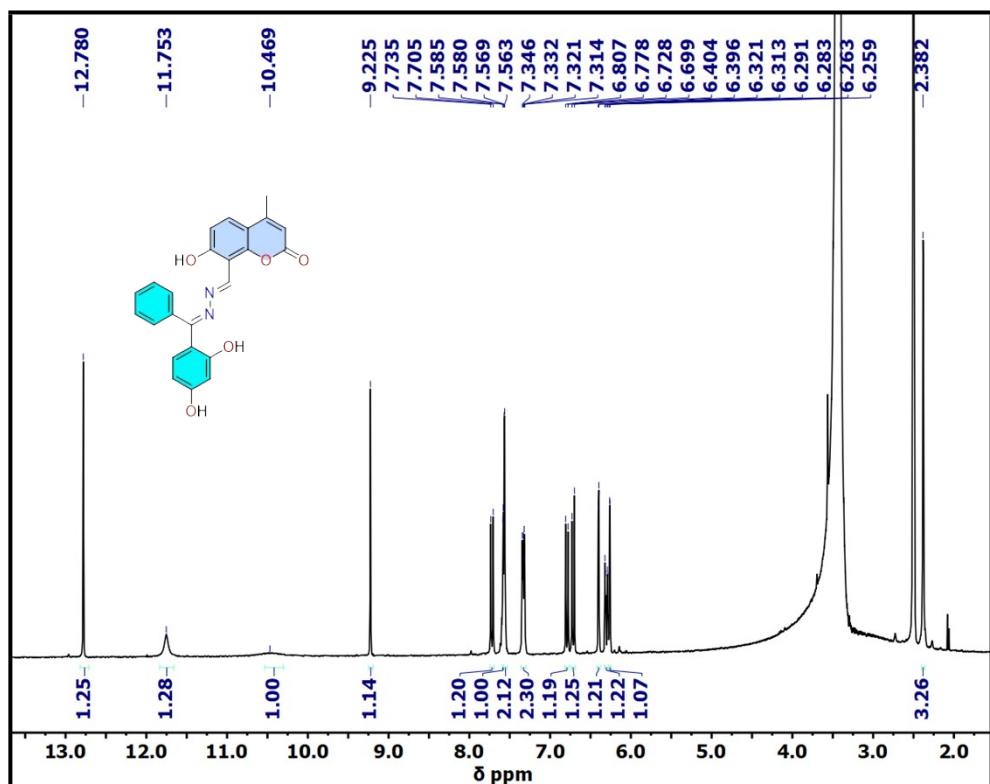


Figure S1: ^1H NMR (300 MHz) spectrum of the probe (DHMH) in DMSO-d_6

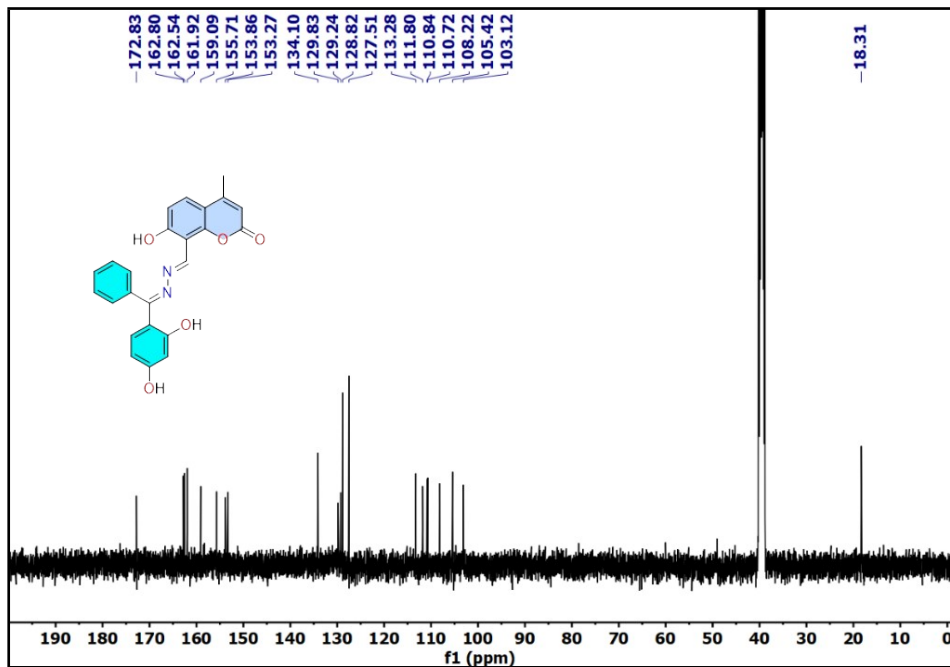


Figure S2: ^{13}C NMR (101 MHz) spectrum of the probe (DHMH) in DMSO-d_6

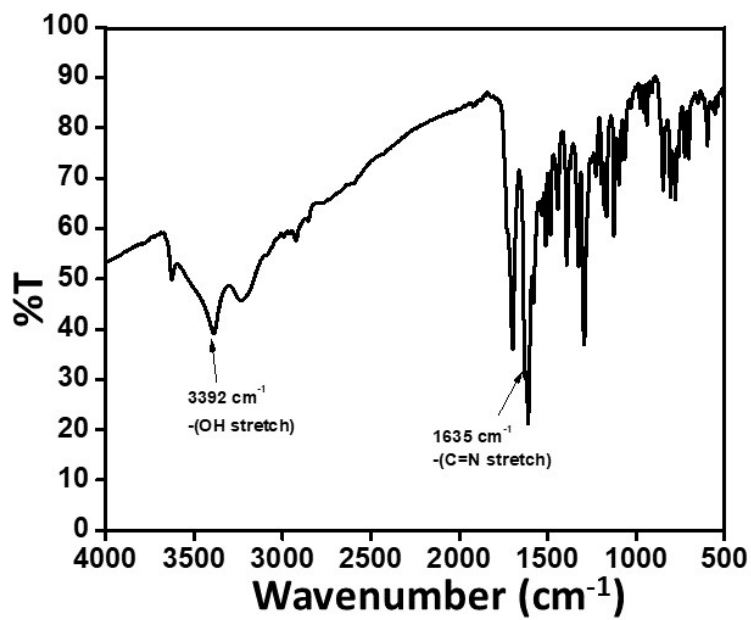


Figure S3: IR plot of the probe (DHMH)

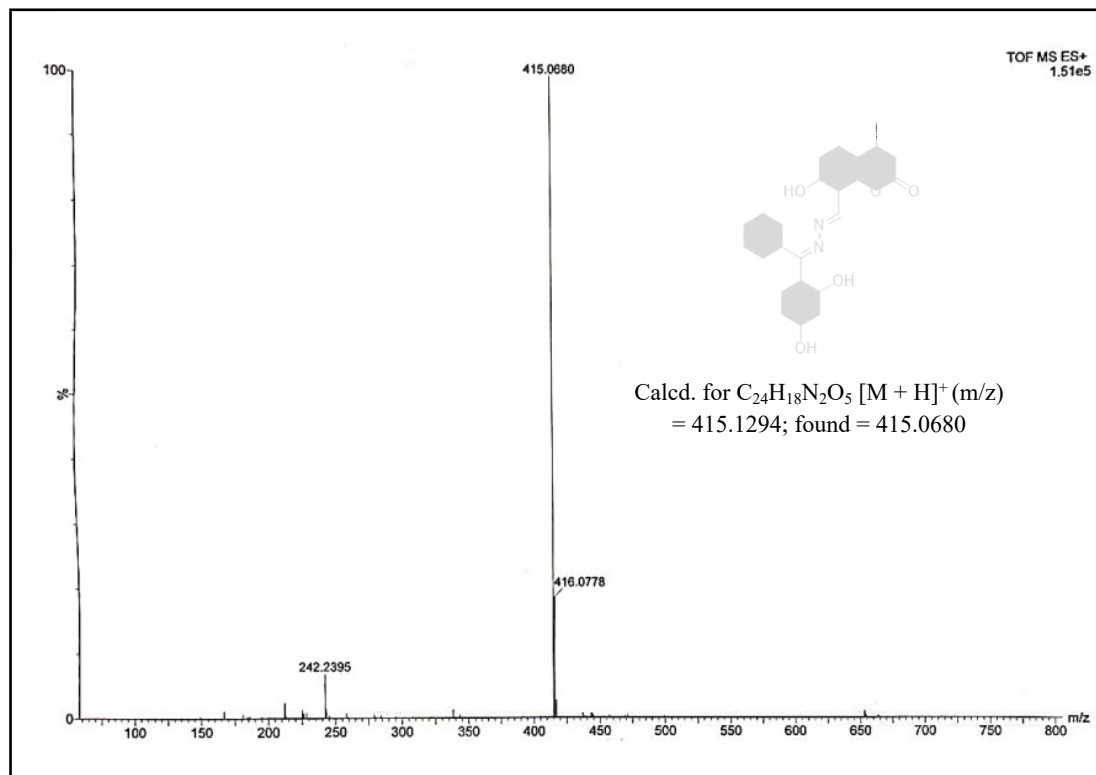


Figure S4: HRMS of the probe DHMH

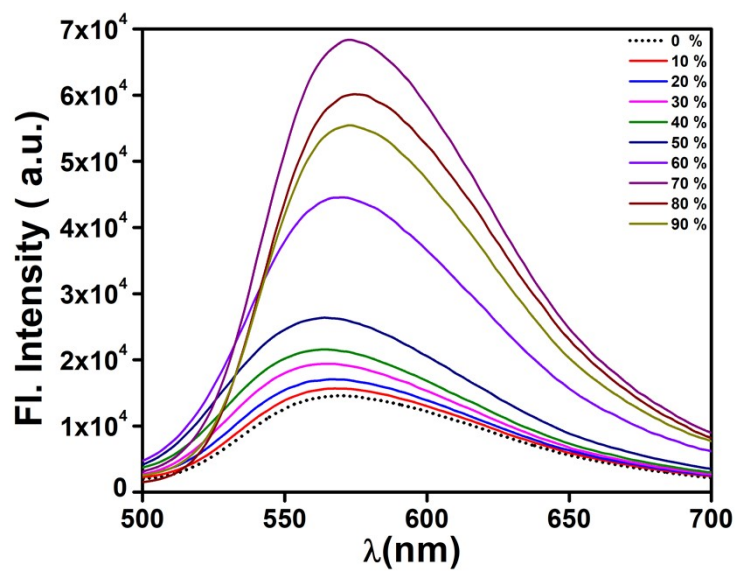


Figure S5: Fluorescence emission spectra of DHMH (10 μM) in DMSO-H₂O mixed solvents with increasing water fractions, excitation at 365 nm.

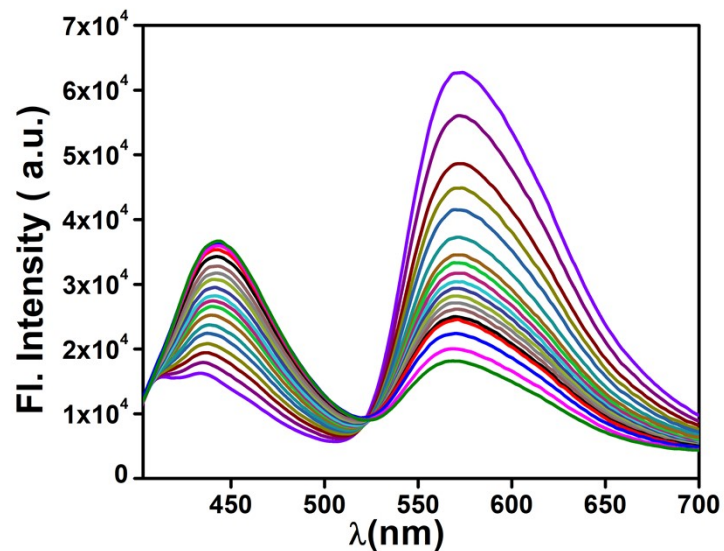


Figure S6: Change of emission spectra of DHMH (10 μM) after addition of CN[−] (20 μM) in DMSO/H₂O (7/3, v/v) using HEPES buffered solution at pH=7.2. $\lambda_{\text{ex}} = 365$ nm.

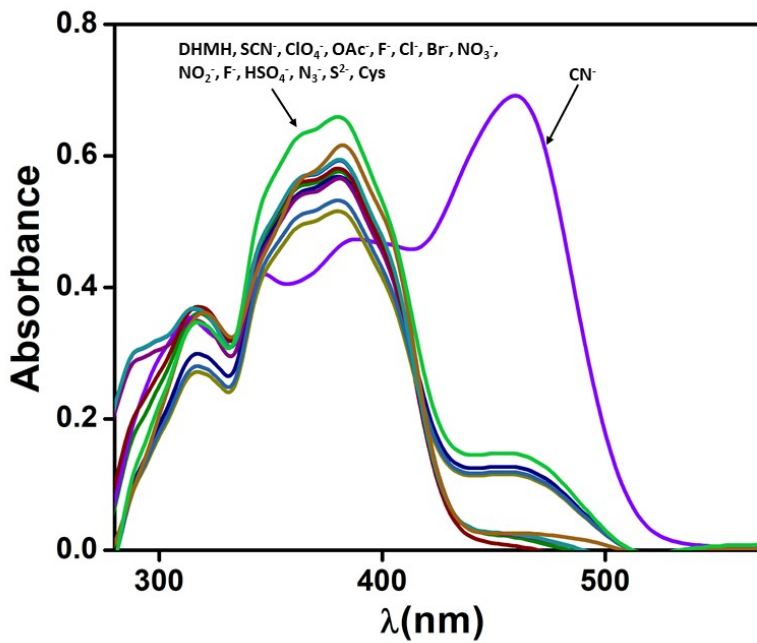


Figure S7: Absorption spectra of DHMH (10 μM) upon addition of various other anions (20 μM) in DMSO/H₂O (9/1, v/v) using HEPES buffered solution at pH=7.2.

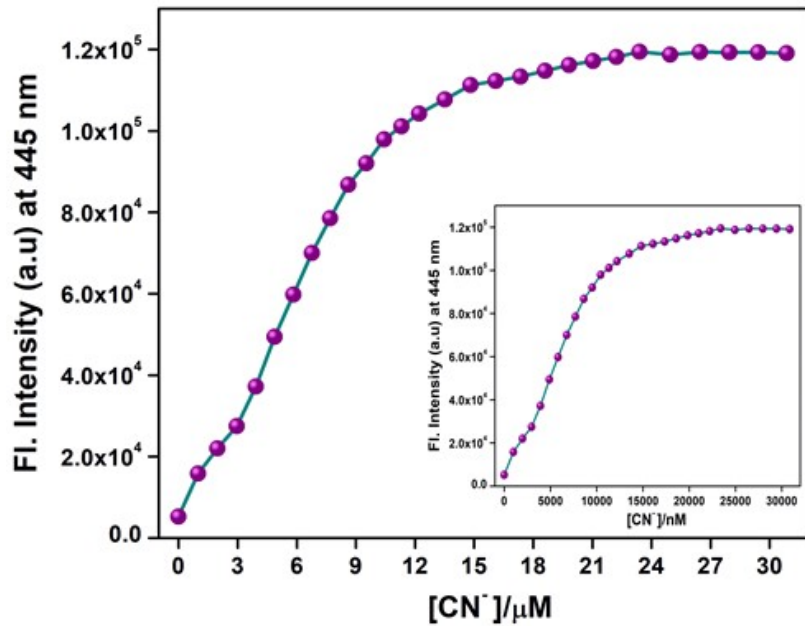


Figure S8: Mole ratio plot of DHMH (10 μM) for CN[−] (20 μM) at 445 nm using fluorescence titration method ($\lambda_{\text{ex}} = 365$ nm).

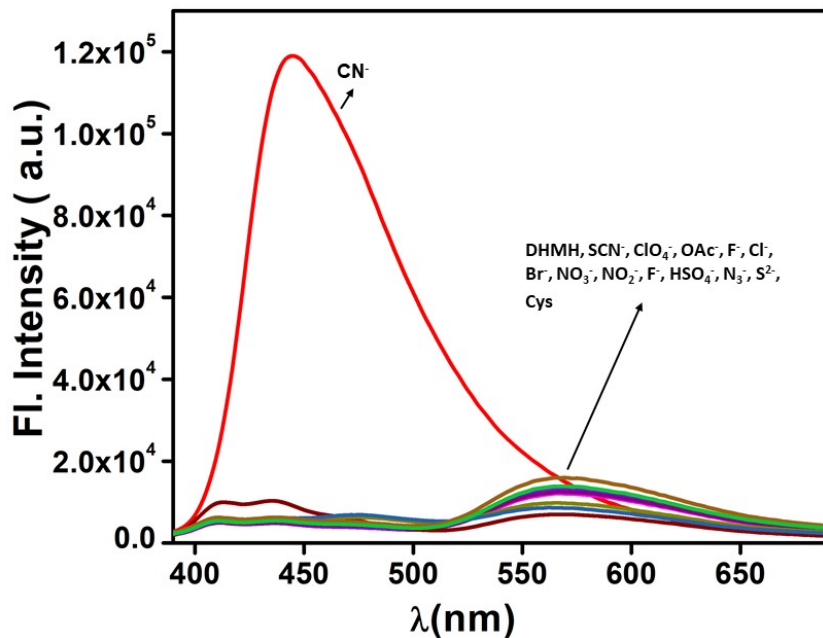


Figure S9: Change of emission spectra of DHMH (10 μM) after addition of other anions (20 μM) in DMSO/H₂O (9/1, v/v) using HEPES buffered solution at pH=7.2. $\lambda_{\text{ex}} = 365$ nm.

Determination of detection limit (LOD)

The limit of detection was determined based on the fluorescence titration. To determine the S/N ratio, the emission intensity of DHMH without CN⁻ was measured by 10 times and the standard deviation of blank measurements was determined. The detection limit of DHMH for CN⁻ was determined from the following equation: $\text{DL} = K \times Sb_1/S$, Where $K = 2$ or 3 (we take 3 in this case); Sb_1 is the standard deviation of the blank solution; S is the slope of the calibration curve.

From the graph we get $SD = 2158.79$ and $slope = 1.01093 \times 10^{10}$. Thus using the formula, we get the Detection Limit = $(0.64 \pm 0.13) \times 10^{-6}$ M i.e., DHMH can detect CN⁻ in this minimum concentration by fluorescence techniques.

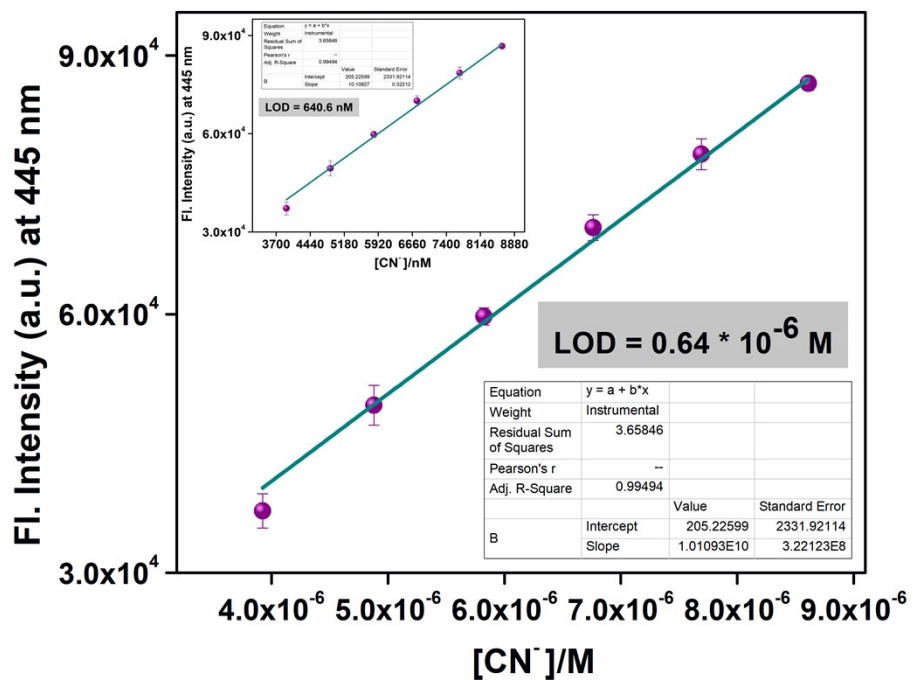
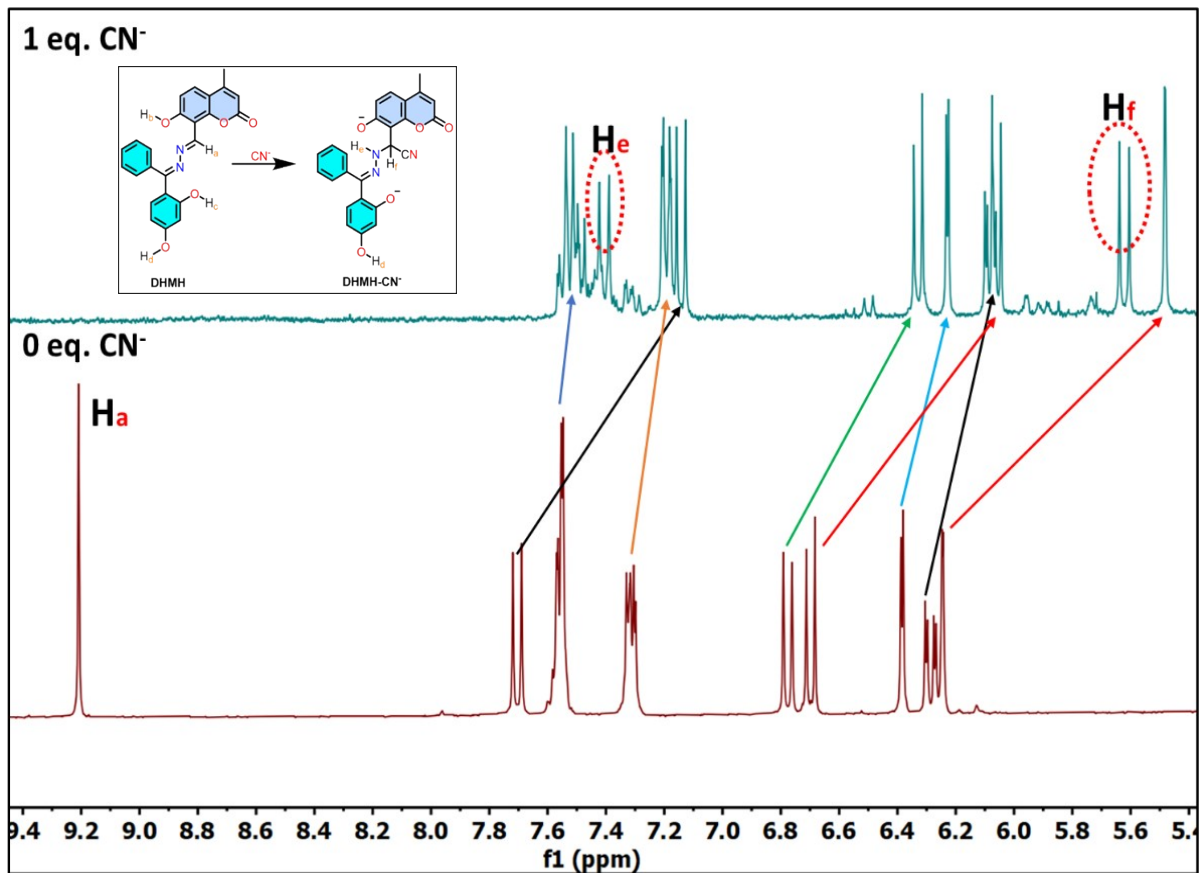


Figure S10: The linear response curve of at emission intensity at 445 nm of DHMH depending on CN^- concentration.



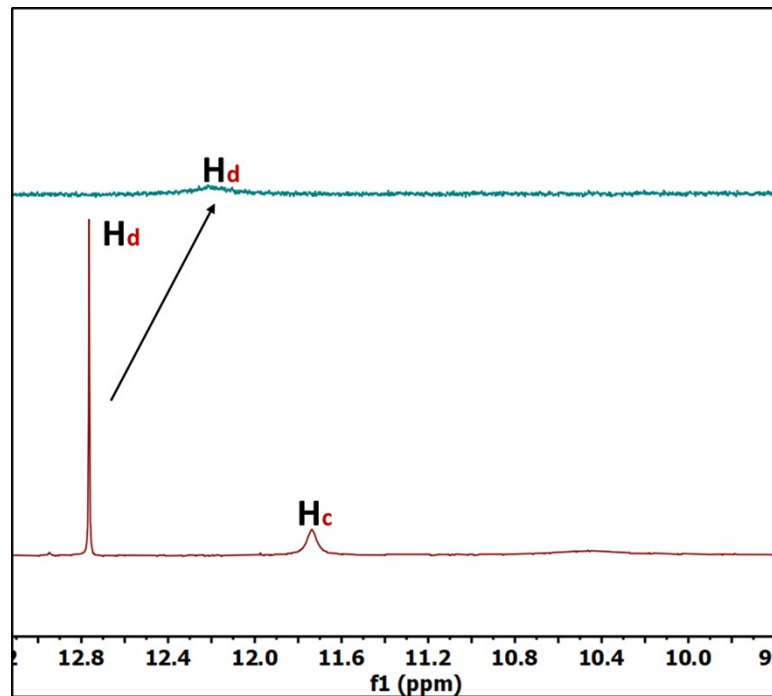


Figure S11: Enlarged ^1H NMR spectra of the probe before and after addition of 1.0 equiv. CN^- in DMSO-d_6 .

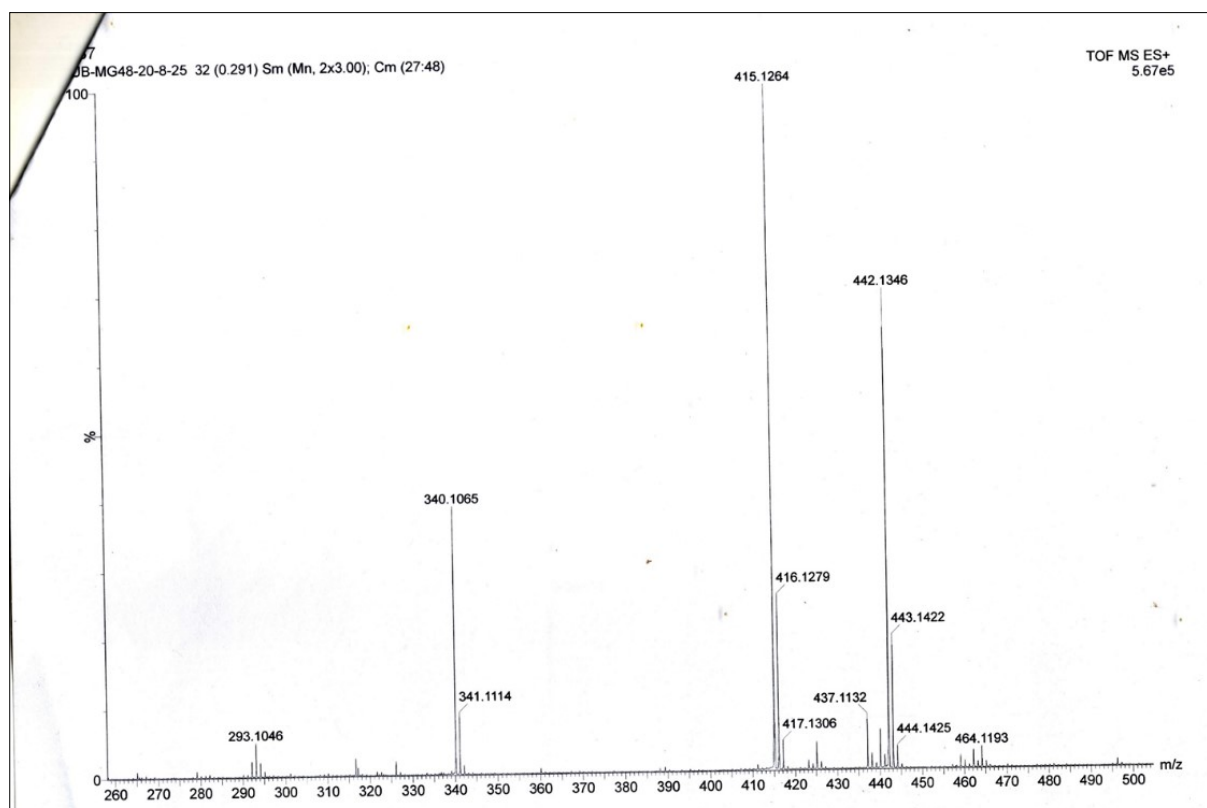


Figure S12: HRMS of DHMH+CN^- .

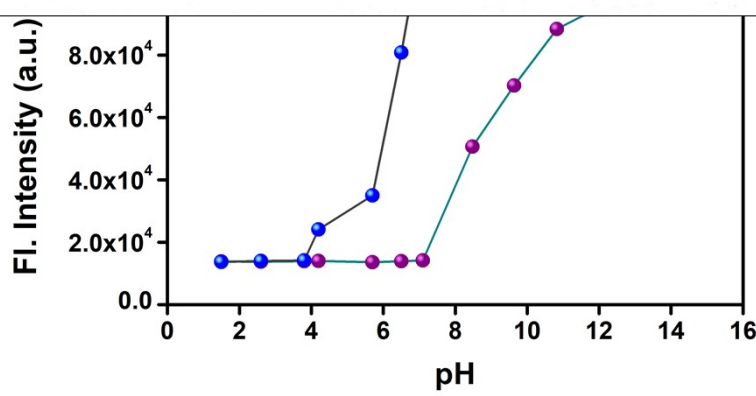


Figure S13: pH titration plot of DHMH and DHMH- CN^- .

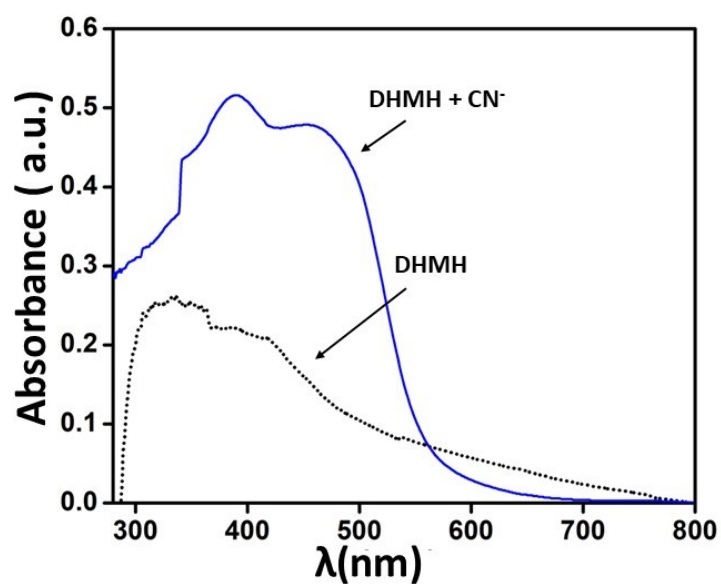


Figure S14: Solid state UV spectral Study of DHMH and DHMH- CN^- by drop-casting method.

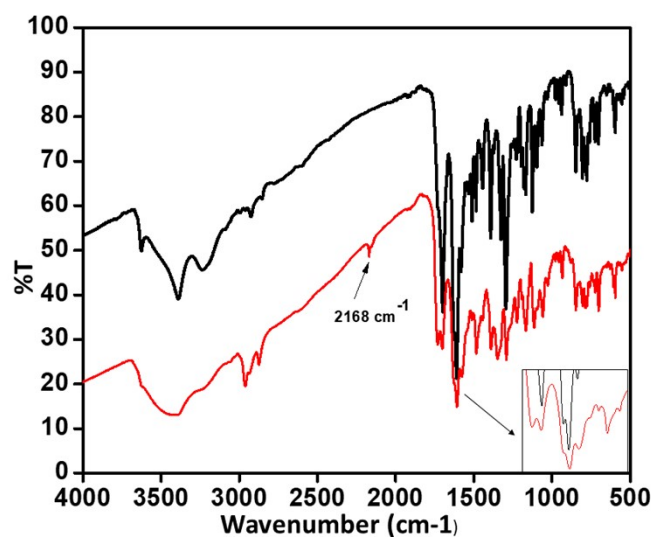


Figure S15: IR spectra of DHMH and DHMH- CN^- .

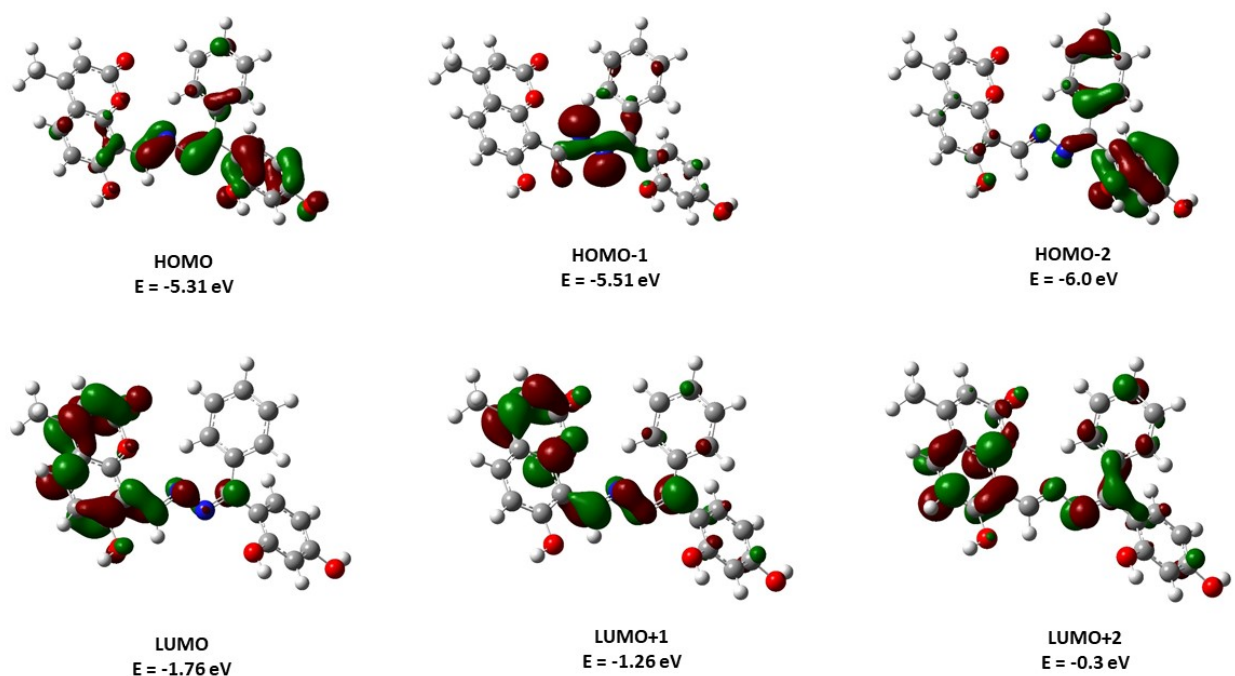


Figure S16. Contour plots of some selected molecular orbitals of DHMH.

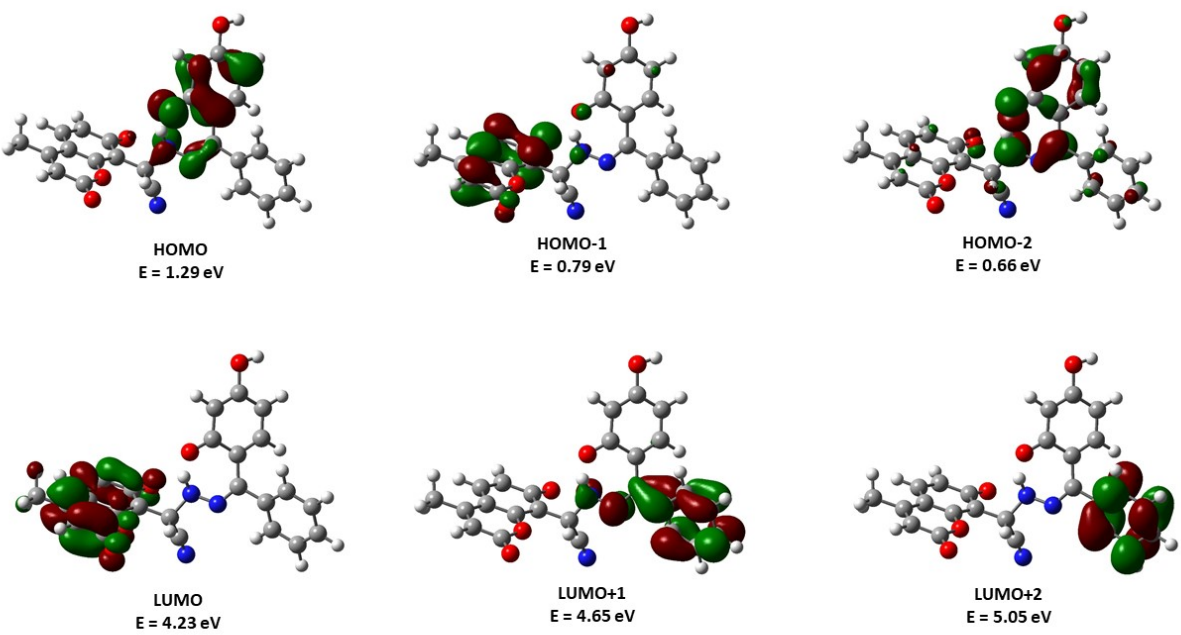


Figure S17. Contour plots of some selected molecular orbitals of DHMH-CN⁻.

Determination of emission quantum yield (Φ) of DHMH and its complex with CN⁻

For measurement of the quantum yields of DHMH and its product with CN⁻ (DHMH-CN⁻), the absorbance of the compounds was recorded in DMSO solution. The emission spectra were then also recorded using the maximal excitation wavelengths and the integrated areas of the emission-corrected spectra were measured. The quantum yields were calculated by comparison with coumarin 153 ($\phi_s = 0.54$ in 0.5M H₂SO₄) as reference using the following equation:

$$\Phi_x = \Phi_s \times \left(\frac{Ix}{Is} \right) \times \left(\frac{As}{Ax} \right) \times \left(\frac{nx}{ns} \right)^2$$

Where, 'x' & 's' designate the unknown and standard solution respectively, Φ is the quantum yield, 'I' refers to the integrated area under the fluorescence spectra, 'A' is the absorbance and 'n' is the refractive index of the solvent. Thus the quantum yields of DHMH and DHMH-CN⁻ were found out to be 0.009 and 0.286 respectively using the above equation.

Table S1. Vertical electronic transitions calculated by TDDFT/B3LYP/CPCM method for DHMH and DHMH-CN⁻ in DMSO

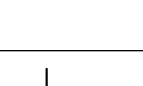
| Compds. | Energy (eV) | Wavelength h (nm) | Osc. strength (f) | Transition | Character |
|---------|-------------|-------------------|-------------------|-------------------|-------------------------------|
| DHMH | 3.2902 | 376.8 | 0.6113 | (88%) HOMO→LUMO | $\pi(L) \rightarrow \pi^*(L)$ |
| | 3.6401 | 340.6 | 0.0994 | (70%) HOMO→LUMO+1 | $\pi(L) \rightarrow \pi^*(L)$ |
| | 3.0827 | 402.2 | 0.0370 | (73%) HOMO-1→LUMO | $\pi(L) \rightarrow \pi^*(L)$ |

| | | | | | |
|-----------------|--------|--------|--------|---------------------|-------------------------------|
| | 3.8066 | 325.7 | 0.1478 | (67%) HOMO-2→LUMO | $\pi(L) \rightarrow \pi^*(L)$ |
| | 3.8915 | 318.6 | 0.1160 | (77%) HOMO-3→LUMO | $\pi(L) \rightarrow \pi^*(L)$ |
| DHMH- | 2.9938 | 414.1 | 0.0064 | (99%) HOMO→LUMO | $\pi(L) \rightarrow \pi^*(L)$ |
| CN ⁻ | 3.2586 | 380.5 | 0.1078 | (94%) HOMO→LUMO+1 | $\pi(L) \rightarrow \pi^*(L)$ |
| (Solution) | 3.4263 | 361.8 | 0.3671 | (94%) HOMO-1→LUMO | $\pi(L) \rightarrow \pi^*(L)$ |
| | 3.5437 | 349.8 | 0.0242 | (95%) HOMO-2→LUMO | $\pi(L) \rightarrow \pi^*(L)$ |
| DHMH- | 2.6702 | 464.33 | 0.0234 | (96%) HOMO→LUMO+4 | $\pi(L) \rightarrow \pi^*(L)$ |
| CN ⁻ | 3.1960 | 387.94 | 0.0417 | (87%) HOMO→LUMO+5 | $\pi(L) \rightarrow \pi^*(L)$ |
| (Solid) | 3.6148 | 342.99 | 0.0346 | (78%) HOMO-1→LUMO+1 | $\pi(L) \rightarrow \pi^*(L)$ |

Table S2: Lifetime decay profile of DHMH and DHMH-CN-

| DMSO (Solvent) | Quantum Yield | τ (ns) | $K_r (10^8 \times S^{-1})$ | $K_{nr} (10^8 \times S^{-1})$ |
|----------------------|---------------|-------------|----------------------------|-------------------------------|
| DHMH | 0.009 | 3.58 | 0.025 | 2.793 |
| DHMH-CN ⁻ | 0.286 | 2.18 | 1.311 | 3.276 |

Table S3: The comparison of the present probe (DHMH) with some previous probes for CN-

| Probe | Type of response | Response Time (min or sec) | Solvent System | Detection limit | Reference |
|---|----------------------|----------------------------|------------------|-----------------|-----------|
|  | Fluorescence turn-on | - | DMSO/MeOH (1:40) | 0.75 μM | [1] |

References:

1. S. Ghosh, S. Paul, S. Halder, M. Shit, A. Karmakar, J. B. Nandi, K. Jana and C. Sinha, *J. Indian Chem. Soc.*, 2023, **100**, 100957.
2. D. Kim, S. Y. Na and H. J. Kim, *Sens. Actuators, B Chem.*, 2015, **220**, 30703.
3. Z. Yang, Z. Liu, Y. Chen, X. Wang, W. He and Y. Lu, *Org. Biomol. Chem.*, 2012, **10**, 5073.
4. B. Yilmaz, M. Keskinates, Z. Aydin and M. Bayrakci, *J. Photochem. Photobiol. A*, 2022, **424**, 113651.
5. P. S. Kumar, P. R. Lakshmi and K. P. Elango, *New J. Chem.*, 2019, **43**, 675.
6. B. B. Wang, Y. Wang, W. N. Wu, Z. H. Xu, X. L. Zhao, Z. Q. Xu and Y. C. Fan, *Inorg. Chem. Commun.*, 2020, **122**, 108245.
7. T. G. Jo, Y. J. Na, J. J. Lee, M. M. Lee, S. Y. Lee and C. A. Kim, *Sens. Actuators, B Chem.*, 2015, **211**, 498.
8. G. H. Liu, Z. Z. Chen, Y. H. Deng and W. K. Dong, *J. Photochem. Photobiol. A Chem.*, 2021, **414**, 113271.
9. M. Nelson, S. Ayyanar, M. Selvaraj and M. A. Assiri, *J. Mol. Struct.*, 2025, **1321**, 140018.